Organic LETTERS

Letter

pubs.acs.org/OrgLett

Synthesis and Divergent Electronic Properties of Two Ring-Fused Derivatives of 9,10-Diphenylanthracene

M. Rajeswara Rao, Hayden T. Black, and Dmitrii F. Perepichka*

Department of Chemistry, McGill University, 801 Sherbrooke Street West, Montreal H3A 0B8, Quebec, Canada

Supporting Information

ABSTRACT: Two new contorted polycyclic aromatic hydrocarbons (PAHs) **1** and **2** were synthesized by acid-catalyzed benzannulation of a substituted anthracene. The isomers reveal dissimilar photophysical and redox properties with **2** having a much smaller HOMO−LUMO gap than **1**. In the solid state, **2** packs in a unique two-dimensional herringbone motif that gives rise to efficient ambipolar charge transport in OFET devices, a feature not previously observed in contorted PAHs. On the other hand, **1** packs in one-dimensional dimerized π-stacks and displays insulating properties.

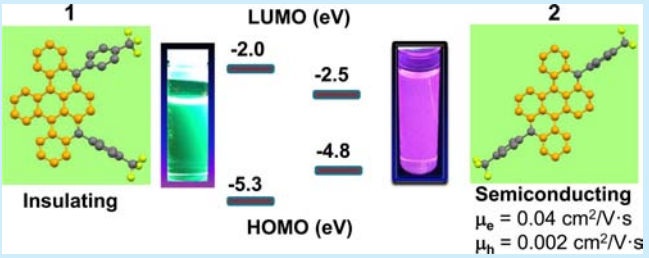

There is a resurgence of interest in polycyclic aromatic hydrocarbons (PAHs) with extended π-systems associated with their special optoelectronic properties and the resulting semiconducting device applications.[1] The extension of PAHs by benzannulation has been utilized as an efficient strategy for tuning the molecular properties and the intermolecular interactions.[2] In many cases, the benzannulation creates steric congestion between the hydrogen atoms of the peripheral aromatic rings resulting in contorted (nonplanar) aromatic structures.[3] Such nonplanar PAHs have a number of important differences versus their flat analogues, which include a significantly enhanced solubility and special self-assembly behavior. Their ability to recognize the convex aromatic surfaces of fullerene derivatives enables some supramolecular control over p−n heterojunction in organic photovoltaics.[4] The "pseudo-3D" π-electron structure of contorted PAH[5] naturally enables multidirectional $\pi-\pi$ contacts which provide pathways for charge carrier hopping in two or even three dimensions. The latter is a highly desirable property for most semiconducting device applications.[6−8]

Herein, we report the synthesis and comparative studies of two contorted PAH isomers derived from electrophilic *syn*- and *anti*-cyclization of substituted 9,10-diphenylanthracene: tribenzopyrene (**1**) and dibenzoperylene (**2**). We show that the two regioisomers display dramatically different photophysical, redox, and solid-state packing properties. As a culmination of these differences, organic field effect transistors (OFETs) fabricated with single crystals of **2** reveal ambipolar charge transport properties, while no measurable conductivity was observed for **1**. We note that relevant (but mechanistically different) cyclizations of diphenylanthracene[9] and diphenylpentacene,[10] to afford rubicene derivatives via 5-membered ring closure, have been reported. The resulting PAHs have been exploited in p-type OFETs showing charge mobilities of 0.2 and 0.06 $cm^2/V{\cdot}s$, respectively. In addition, the unsubstituted tribenzopyrene[11] and dibenzoperylene[12] representing the same π-system as **1** and **2** are known, but their studies were limited to characterization of the photooxidation.[12]

With the prospect of isolating two isomers in one reaction, we originally commenced our synthesis (Scheme 1) from di(2-formylphenyl)anthracene[13] **3**, prepared via standard Suzuki−Miyaura cross-coupling of 9,10-dibromoanthracene with 2-formylphenylboronic acid. Nucleophilic addition of two equiv of *p*-CF_3PhLi to **3** gave the tertiary dialcohol **4**. Subsequent acid-catalyzed intramolecular cyclization of crude **4** in neat trifluoroacetic acid (TFA) in air is accompanied by spontaneous oxidative aromatization and affords a ∼100:1 mixture of **1** and **2** in 48% yield. The isomers were easily separable via physical vapor transport (PVT) at 150 °C. However, all attempts to increase the amount of **2** by changing the catalyst (HCl, TFA, and $BF_3{\cdot}Et_2O$), temperature, or concentration of the reaction, met with no success. The high regioselectivity to form *syn* isomer **1** can be rationalized by the orientation effect of the electron-donating $-CHAr_2$ group introduced during the closure of the first ring.

In order to produce a sufficient amount of **2**, we planned to involve the diketo intermediate **6**, which was expected to be a preferred product of intramolecular Friedel−Crafts cyclization of 9,10-di(2-carboxyphenyl)anthracene. However, an attempted oxidation of the sterically congested dialdehyde **3** turned out to be ill-defined, and the corresponding dicarboxylic acid could not be isolated. Instead, **6** was synthesized by rearrangement of dilactone **5** in polyphosphoric acid as proposed earlier[14] (**5** is prepared by reaction of anthraquinone with 2,*N*-dilithiated *N*-methylbenzamide). The nucleophilic addition of *p*-CF_3PhLi to the diketone **6** resulted in the tertiary dialcohol **7** which was aromatized by treatment with $SnCl_2$ to finally afforded **2**.[15] Both isomers are readily soluble in common organic solvents

Received: July 13, 2015
Published: August 18, 2015

DOI: 10.1021/acs.orglett.5b02009
Org. Lett. 2015, 17, 4224−4227

Scheme 1. Synthesis of PAH Isomers 1 and 2

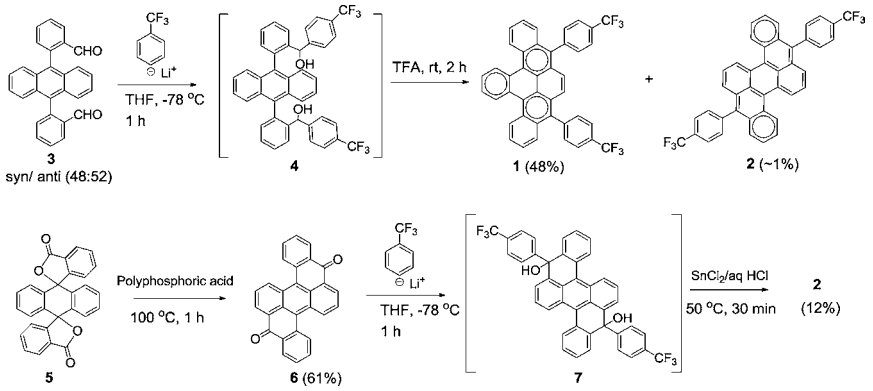

($CHCl_3$, THF, etc.). In solution, **2** is prone to rapid photooxidation (half-life of <30 min) in ambient light conditions, as previously shown for unsubstituted dibenzoperylene,[12] and commonly observed for most acenes longer than tetracene.[16] This is not, however, the case for **1** (see the Supporting Information). Both compounds are stable in the solid state.

The absorption and emission bands of both isomers feature distinct vibronic splitting (~1300 cm^{-1}), typical for many PAHs (Figure 1). The lowest energy absorption maximum of **2**

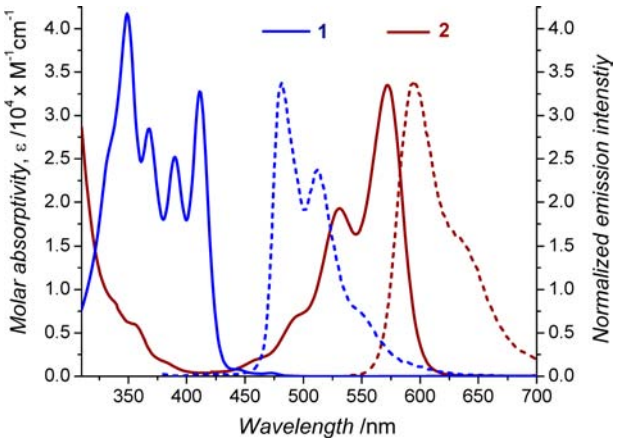

Figure 1. Absorption and emission spectra of **1** and **2** recorded in CH_2Cl_2.

(571 nm) is significantly red-shifted compared to **1** (410 nm[17]). The TD-DFT calculations (B3LYP 6-31/G(d)) reproduce this trend well, predicting the first electronic transitions at 596 nm for **2** (oscillator strength, f = 0.47) and at 416 nm for **1** (f = 0.41). The rational for the observed behavior can be derived from Clar's aromatic sextet rule.[18] According to Clar, the presence of three disjoint sextets in the structure of **1**, compared to two sextets in **2** (Scheme 1), would lead to higher aromaticity and stability but also lower π-electron delocalization between the individual benzene rings. The optical gap estimated from the maximum of the first vibronic peak is 2.17 eV for **2** and 3.02 eV for **1**.

In solution, both isomers display red and greenish-blue fluorescence with the quantum yields of 0.9% and 0.5% for **2** and **1**, respectively (Figure 1). The weak emissivity is likely due to the conformational freedom of their contorted backbones (out-of-plane deformation) which facilitates nonradiative relaxation. The relatively large Stokes shift (706 cm^{-1} for **2** and 3540 cm^{-1} for **1**) could be understood in terms of partial planarization of the excited state. The higher polarity of noncentrosymmetric **1** (net dipole moment 4.7 D according to DFT) might be also responsible for its large Stokes shift. In the solid state, **1** shows a red-shifted weak emission (λ_{max} = 518 nm, Supporting Information), while **2** is nonemissive.

The electrochemical properties were measured in CH_2Cl_2 solution by cyclic voltammetry (Figure 2). Both isomers

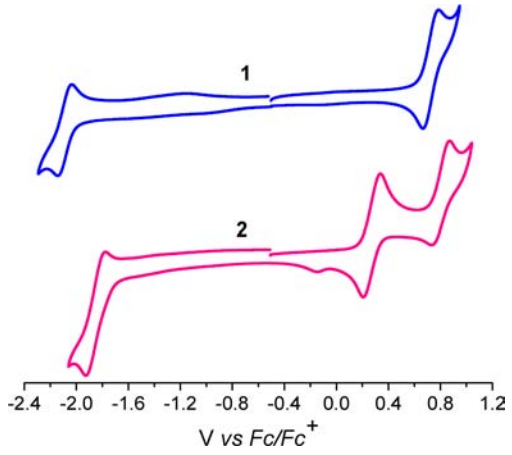

Figure 2. Cyclic voltammograms of **1** and **2** in 0.2 M Bu_4NPF_6 in CH_2Cl_2; reduction of **1** was recorded in DMF.

undergo reversible single-electron oxidation and reduction waves, and a second partially reversible oxidation wave was also observed for **2**. The latter is easier to both oxidize and reduce as compared to **1**, in accord with its lower HOMO−LUMO gap (**2**: $E^{1/2}_{ox}$ = 0.29 V vs Fc/Fc^+ and $E^{1/2}_{red}$ = −1.83 V; **1**: $E^{1/2}_{ox}$ = 0.75 V; $E^{1/2}_{red}$ = −2.08 V). The electrochemical gaps of 2.8 eV for **1** and 2.1 eV for **2** are quite similar to the optical gaps determined from the absorption spectra. Assuming Fc/Fc^+ at −4.8 eV vs vacuum, the HOMO of −5.55 and −5.09 eV and LUMO of −2.72 and −2.98 eV were determined for **1** and **2**, respectively. This trend is in line with the DFT calculations (HOMOs: −5.27/−4.78 eV and LUMOs: −2.04/−2.54 eV for **1** and **2**, respectively).

Single crystals of **1** and **2** were grown via physical vapor transport at 150 °C, as yellow needles and red plates, respectively. Their X-ray crystallographic analysis reveals triclinic (P-1) and orthorhombic ($Pbca$) space groups for **1** and **2**, respectively. Compound **1** adopts a saddle conformation in which peripheral rings A are tilted vs each other by 43° and protrude above the anthracene core BCD (Figure 3). The latter

DOI: 10.1021/acs.orglett.5b02009
Org. Lett. 2015, 17, 4224−4227

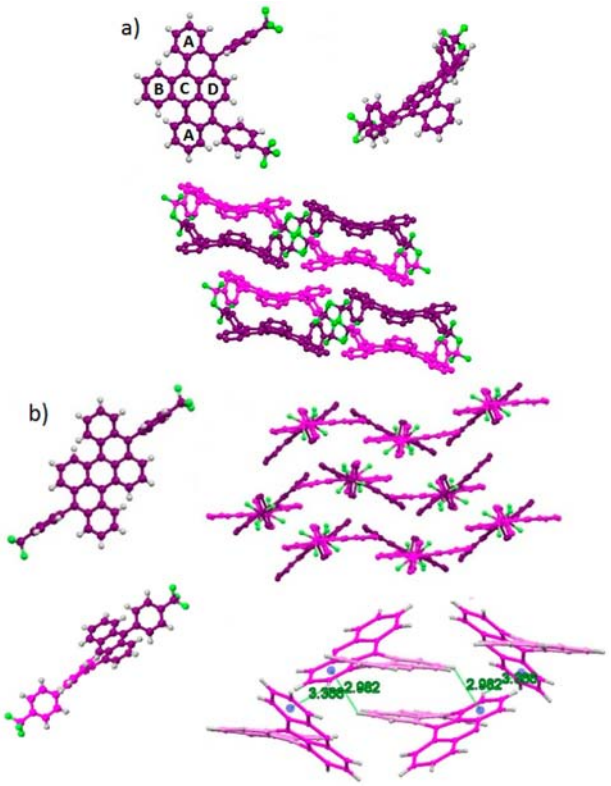

Figure 3. Crystal structures and molecular packing diagrams of **1** (a) and **2** (b).

is also curved: the interplanar angle of the ring B vs D is 34°. Compound **2** is twisted in a propeller conformation: the two *p*-CF_3Ph-substituted anthracene moieties rotate vs each other by 31.5°, while the said moieties are nearly planar (6.8° angle between their terminal benzene rings). A similar conformation was observed for tetrachloroperylenedimide.[5a] In both **1** and **2**, the *p*-CF_3Ph substituents are rotated out of plane by 60−73° and thus do not contribute significantly to the electron π-delocalization, except by inductive effect. The observed molecular geometry matches well that predicted by DFT (Supporting Information).

In the crystal of **1**, two molecules form cofacial antiparallel pairs with two identical C−C short contacts of 3.37 Å. These pairs stack further into a one-dimensional slipped π-stack; the closed $\pi\cdots\pi$ contacts between the dimers of the stack are 3.79 Å. Such dimerized packing motif is not expected to provide efficient conductivity channels.

Compound **2** adopts an unusual intermolecular packing, where each side of the twisted molecule affords a herringbone-like structure with anthracene moiety of neighboring molecule. This creates a two-dimensional network of close π-interactions (3.37−3.41 Å), an essential feature of most high mobility molecular semiconductors.[19]

Single-crystal field effect transistors were fabricated in order to study the charge-transport properties of the two isomers. A bottom-gate top-contact device configuration was employed where PVT-grown crystals were laminated on Si/SiO_x substrate with thin polystyrene adhesion layer and gold source/drain electrodes were patterned atop via shadow-mask evaporation (Figure 4a,b). OFET with **1** did not show any gate response, and the unobservable low conductivity ($<10^{-8}$ S/cm) reveals an insulating behavior. The inefficient charge transport in **1** could

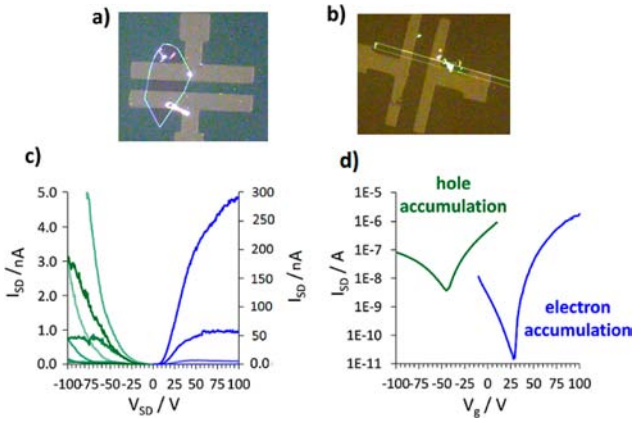

Figure 4. Optical image of single crystal transistor fabricated with **2** (a) and **1** (b). Output characteristics (c) and transfer characteristics (d) of the OFET fabricated with **2** (L = 30 μm; W = 100 μm).

be attributed to the lack of percolating π-interactions due to dimerized packing motif. In contrast, OFET using **2** displayed an ambipolar behavior (Figure 4c,d), with maximum charge mobilities of μ_h = 0.002 $cm^2/V\cdot s$ and μ_e = 0.04 $cm^2/V\cdot s$. These values are most likely limited by the substantial contact resistance, which is evident from a sigmoidal shape of the output characteristics in both *p*- and *n*- channels (Figure 4c). The relatively efficient electron transport in **2** was surprising, considering the large mismatch of the Au work function (−5.2 eV) with LUMO (comparing to HOMO, see above). It is likely attributable to trifluoromethyl substituents that can perturb the interfacial energetics, due to dipole-induced changes to the work function of the Au electrodes, and also minimize the electron trapping by expelling water impurities from the interface (hydrophobic effect).[20]

We should note that the achieved charge mobilities are not among the highest observed in contorted PAH. Thus, hole mobilities up to 0.9 $cm^2/V\cdot s$ have been reported for contorted hexabenzocoronene derivatives.[6] Also, electron mobilities up to 1 $cm^2/V\cdot s$ have been measured for contorted octachloroperylenediimide.[5c,d] Fullerene C_{60}, although not considered aromatic, can show even higher electron mobility up to 11 $cm^2/V\cdot s$.[21] However, a simultaneous hole and electron (ambipolar) transport in OFET with standard, high work-function electrodes (Au) is more rare[22] but important, e.g., for logic circuits[23] and light-emitting transistors[24] applications. To our knowledge, it has not been previously reported in contorted PAH, although either hole or electron transport can be enforced in such materials by engineering the injection barrier, as was shown, *eg.* in twistacene based diodes.[25]

In summary, we have reported the synthesis of two PAHs by acid-catalyzed cyclization of 9,10-diphenylanthracene derivatives. The isomeric products tribenzopyrene (**1**) and dibenzoperylene (**2**) reveal dramatically different photophysical and electrochemical properties and photostability. These are connected with the better electron delocalization and lower HOMO−LUMO gap of **2** that are predicted by Clar's sextet rule. X-ray crystallography shows a highly contorted structure for both molecules which pack in either one-dimensional stacks of "sandwich pairs" (for **1**) or a two-dimensional herringbone arrangement (for **2**). The crystals of **2** afford an ambipolar OFET device with hole mobility of 0.002 $cm^2/V\cdot s$ and electron mobility of 0.04 $cm^2/V\cdot s$, while **1** displays an insulating behavior. While these charge mobilities are ∼3 orders of

DOI: 10.1021/acs.orglett.5b02009
Org. Lett. 2015, 17, 4224−4227

magnitude lower than the record values for organic semiconductors, they are sufficiently high for a number of device applications. In particular, the contorted π-electron structure and associated 3D interactions in the solid state are of great interest for organic photovoltaics,[4,8] and the ability to effectively synthesize such compounds from simple building blocks (anthracene) paves the way for a new class of tailored semiconducting materials.

■ ASSOCIATED CONTENT

Supporting Information

The Supporting Information is available free of charge on the ACS Publications website at DOI: 10.1021/acs.orglett.5b02009.

Synthetic procedures and spectroscopic data of the synthesized compounds; additional computational, crystallographic, and photophysical details (PDF)
Crystallographic data for **1** (CIF)
Crystallographic data for **2** (CIF)

■ AUTHOR INFORMATION

Corresponding Author

*E-mail: dmitrii.perepichka@mcgill.ca.

Notes

The authors declare no competing financial interest.

■ ACKNOWLEDGMENTS

This work was supported by NSERC of Canada and NanoQuebec. M.R.R. thanks FQRNT for PBEEE fellowship.

■ REFERENCES

(1) (a) Bendikov, M.; Wudl, F.; Perepichka, D. F. *Chem. Rev.* **2004**, *104*, 4891−4945. (b) Anthony, J. E. *Chem. Rev.* **2006**, *106*, 5028−5048. (c) Figueira-Duarte, T. M.; Müllen, K. *Chem. Rev.* **2011**, *111*, 7260−7314. (d) Mateo-Alonso, A. *Chem. Soc. Rev.* **2014**, *43*, 6311−6324.

(2) (a) Sun, Z.; Ye, Q.; Chi, C.-Y.; Wu, J.-S. *Chem. Soc. Rev.* **2012**, *41*, 7857−7889. (b) Shen, Y.; Chen, C.-F. *Chem. Rev.* **2012**, *112*, 1463−1535.

(3) (a) Pascal, R. A. *Chem. Rev.* **2006**, *106*, 4809−4819. (b) Eversloh, C. L.; Liu, Z.; Müller, B.; Stangl, M.; Li, C.; Müllen, K. *Org. Lett.* **2011**, *13*, 5528−5531. (c) Zöphel, L.; Enkelmann, V.; Rieger, R.; Müllen, K. *Org. Lett.* **2011**, *13*, 4506−4509. (d) Arslan, H.; Uribe-Romo, F. J.; Smith, B. J.; Dichtel, W. R. *Chem. Sci.* **2013**, *4*, 3973−3978. (e) Ball, M.; Zhong, Y.; Wu, Y.; Schenck, C.; Ng, F.; Steigerwald, M.; Xiao, S.; Nuckolls, C. *Acc. Chem. Res.* **2015**, *48*, 267−276.

(4) (a) Tremblay, N. J.; Gorodetsky, A. A.; Cox, M. P.; Schiros, T.; Kim, B.; Steiner, R.; Bullard, Z.; Sattler, A.; So, W.-H.; Itoh, Y.; Toney, M. F.; Ogasawara, H.; Ramirez, A. P.; Kymissis, I.; Steigerwald, M. L.; Nuckolls, C. *ChemPhysChem* **2010**, *11*, 799−803. (b) Xiao, S.; Kang, S. J.; Wu, Y.; Ahn, S.; Kim, J. B.; Loo, Y.-L.; Siegrist, T.; Steigerwald, M. L.; Li, H.; Nuckolls, C. *Chem. Sci.* **2013**, *4*, 2018−2023.

(5) (a) Chen, Z.; Debije, M. G.; Debaerdemaeker, T.; Osswald, P.; Würthner, F. *ChemPhysChem* **2004**, *5*, 137−140. (b) Gsänger, M.; Oh, J. H.; Könemann, M.; Höffken, H. W.; Krause, A.-M.; Bao, Z.; Würthner, F. *Angew. Chem., Int. Ed.* **2010**, *49*, 740−743. (c) Ling, M. M.; Erk, P.; Gomez, M.; Könemann, M.; Locklin, J.; Bao, Z. *Adv. Mater.* **2007**, *19*, 1123−1127. (d) Schmidt, R.; Oh, J. H.; Sun, Y.-S.; Deppisch, M.; Krause, A.-M.; Radacki, K.; Braunschweig, H.; Könemann, M.; Erk, P.; Bao, Z.; Würthner, F. *J. Am. Chem. Soc.* **2009**, *131*, 6215−6228.

(6) Xiao, S.; Myers, M.; Miao, Q.; Sanaur, S.; Pang, K.; Steigerwald, M. L.; Nuckolls, C. *Angew. Chem., Int. Ed.* **2005**, *44*, 7390−7394.

(7) (a) Zhang, X.; Jiang, X.; Luo, J.; Chi, C.; Chen, H.; Wu, J. *Chem. - Eur. J.* **2010**, *16*, 464−468. (b) Lv, A.; Puniredd, S. R.; Zhang, J.; Li, Z.; Zhu, H.; Jiang, W.; Dong, H.; He, Y.; Jiang, L.; Li, Y.; Pisula, W.; Meng, Q.; Hu, W.; Wang, Z. *Adv. Mater.* **2012**, *24*, 2626−2630. (c) Skabara, P. J.; Arlin, J.-B.; Geerts, Y. H. *Adv. Mater.* **2013**, *25*, 1948−1954.

(8) Brunetti, F. G.; Gong, X.; Tong, X.; Heeger, A. J.; Wudl, F. *Angew. Chem., Int. Ed.* **2010**, *49*, 532−536.

(9) (a) Smet, M.; Shukla, R.; Fülöp, L.; Dehaen, W. *Eur. J. Org. Chem.* **1998**, 2769−2773. (b) Lee, H.; Zhang, Y.; Zhang, L.; Mirabito, T.; Burnett, E. K.; Trahan, S.; Mohebbi, A. R.; Mannsfeld, S. C. B.; Wudl, F.; Briseno, A. L. *J. Mater. Chem. C* **2014**, *2*, 3361−3366.

(10) Lakshminarayana, A. N.; Chang, J.; Luo, J.; Zheng, B.; Huang, K.-W.; Chi, C. *Chem. Commun.* **2015**, *51*, 3604−3607.

(11) Harvey, R. G.; Yang, D. T. C.; Yang, C. *Polycyclic Aromat. Compd.* **1994**, *4*, 127−133.

(12) Kajiwara, T.; Fujisawa, S.; Ohno, K.; Harada, Y. *Bull. Chem. Soc. Jpn.* **1979**, *52*, 2771−2777.

(13) Zehm, D.; Fudickar, W.; Hans, M.; Schilde, U.; Kelling, A.; Linker, T. *Chem. - Eur. J.* **2008**, *14*, 11429−11441.

(14) Carissimo-Rietsch, F.; Schmitz, C.; Aubry, J.-M. *Tetrahedron Lett.* **1991**, *32*, 3845−3846.

(15) Besides **2**, an unexpected formation of the triarylated compound (5%) was also noticed. This, as well as a partial decomposition (likely photooxidation) of **2** during purification by column chromatography, led to the low isolated yield. The characterization of the triarylated product will be reported elsewhere.

(16) (a) Reddy, A. R.; Bendikov, M. *Chem. Commun.* **2006**, 1179−1181. (b) Zade, S. S.; Bendikov, M. *J. Phys. Org. Chem.* **2012**, *25*, 452−461. (c) Kaur, I.; Jia, W.; Kopreski, R. P.; Selvarasah, S.; Dokmeci, M. R.; Pramanik, C.; McGruer, N. E.; Miller, G. P. *J. Am. Chem. Soc.* **2008**, *130*, 16274−16286. (d) Zhang, J.; Sarrafpour, S.; Haas, T. E.; Müller, P.; Thomas, S. W., III *J. Mater. Chem.* **2012**, *22*, 6182−6189.

(17) Compound **1** also shows a weak absorption band with λ_{max} = 442 and 473 nm (see the Supporting Information). These peaks remain unchanged after multiple purification steps, and they are also seen in the excitation spectrum. This could possibly be attributed to a minor conformer. Indeed, DFT predicts a local minimum with C_2 symmetry at +5.2 kcal/mol relative to the lowest energy conformer (with σ-symmetry). TD-DFT calculations on this conformer suggest a red-shifted absorption (Supporting Information).

(18) Solà, M. *Front. Chem.* **2013**, *1:22*, 1−8.

(19) Mas-Torrent, M.; Rovira, C. *Chem. Rev.* **2011**, *111*, 4833−4856.

(20) Facchetti, A.; Deng, Y.; Wang, A. C.; Koide, Y.; Sirringhaus, H.; Marks, T. J.; Friend, R. H. *Angew. Chem., Int. Ed.* **2000**, *39*, 4547−4551.

(21) Li, H.; Tee, B. C.-K.; Cha, J. J.; Cui, Y.; Chung, J. W.; Lee, S. Y.; Bao, Z. *J. Am. Chem. Soc.* **2012**, *134*, 2760−2765.

(22) Zhao, Y.; Guo, Y.; Liu, Y. *Adv. Mater.* **2013**, *25*, 5372−5391.

(23) (a) Crone, B.; Dodabalapur, A.; Lin, Y.-Y.; Filas, R. W.; Bao, Z.; LaDuca, A.; Sarpeshkar, R.; Katz, H. E.; Li, W. *Nature* **2000**, *403*, 521−523. (b) Ryu, H.; Kälblein, D.; Weitz, R. H.; Ante, F.; Zschieschang, U.; Kern, K.; Schmidt, O. G.; Klauk, H. *Nanotechnology* **2010**, *21*, 475207.

(24) (a) Capelli, R.; Toffanin, S.; Generali, G.; Usta, H.; Facchetti, A.; Muccini, M. *Nat. Mater.* **2010**, *9*, 496−503. (b) Dadvand, A.; Moiseev, A. G.; Sawabe, K.; Sun, W.-H.; Djukic, B.; Chung, I.; Takenobu, T.; Rosei, F.; Perepichka, D. F. *Angew. Chem., Int. Ed.* **2012**, *51*, 3837−3841.

(25) Zhang, Q.; Divayana, Y.; Xiao, J.; Wang, Z.; Tiekink, E. R. T.; Doung, H. M.; Zhang, H.; Boey, F.; Sun, X. W.; Wudl, F. *Chem. - Eur. J.* **2010**, *16*, 7422−7426.

DOI: 10.1021/acs.orglett.5b02009
Org. Lett. 2015, 17, 4224−4227